

Investigation of trapping/detrapping mechanisms in Al_2O_3 electron/hole traps and their influence on TANOS memory operations

Luca Larcher¹, Andrea Padovani¹, Vincenzo della Marca², Paolo Pavan², Alessandro Bertacchini¹

¹DISMI, Università di Modena e Reggio Emilia, and IU.NET, Via Amendola 2, 42122 Reggio Emilia, Italy

²DII, Università di Modena e Reggio Emilia, and IU.NET, Via Vignolese 905, 41100 Modena, Italy

luca.larcher@unimore.it

Alumina is a key material for developing innovative Charge-Trapping Non-Volatile Memory (CT-NVM) devices. Al_2O_3 is used to implement the top dielectric in TANOS devices [1], and it has been proposed as trapping layer [2] and to engineer the tunnel dielectric [3]. Despite the large use of this material, the quantitative investigation of defect features still lacks. In this scenario, the purpose of this work is to investigate the physics of electron/hole trapping/detrapping mechanisms in Al_2O_3 . Combining I-V and C-V measurements with a physical model we derive the energy levels of electron/hole traps and the location of electron/hole charge. The influence of electron/hole alumina traps on TANOS operations and reliability is investigated.

We developed a combined I-V and C-V measurement scheme: 1) C-V on fresh device; 2) I-V measure performed applying a gate voltage V_G ramp (0.1V/s) from 0 to $V_{G,\text{MAX}}$; 3) C-V; 4) I-V varying V_g from $V_{G,\text{MAX}}$ to $V_{G,\text{MIN}}$; 5) C-V; 6) I-V varying V_G from $V_{G,\text{MIN}}$ to 0. $V_{G,\text{MAX}}$ and $V_{G,\text{MIN}}$ are selected to limit the maximum current density to $\sim 100 \text{ mA/cm}^2$ in order to prevent the dielectric breakdown. Devices used are large area ($\sim 9.18 \times 10^{-3} \text{ cm}^2$) n-MOS capacitors with TiN/ Al_2O_3 / SiO_2 /Si stack, manufactured using standard process. Alumina thicknesses are $t_{\text{Al}}=5, 10$ and 15 nm , with a thin ($\sim 1 \text{ nm}$) interfacial SiO_x layer at the Si interface. Thicknesses and relative dielectric constants of interfacial SiO_x ($k_{\text{SiO}_x}=5$ [5]) and Al_2O_3 ($k_{\text{Al}_2\text{O}_3}=9.15$) layers are extracted from C-V measurements. Fig. 1 shows C-V curves measured on samples with $t_{\text{Al}}=15 \text{ nm}$. Simulations performed using the model in [6] reproduce accurately the measurements. For virgin devices, we assumed a fixed electron charge density $\sim 10^{12} \text{ e/cm}^2$ at the $\text{SiO}_x/\text{Al}_2\text{O}_3$ interface, attributed to the process. Fig. 2 shows I-V curves measured on the $t_{\text{Al}}=15 \text{ nm}$ capacitor. I-V characteristics show a significant hysteresis especially at positive V_G , indicating that electron trapping occurs during the $V_G=0-16 \text{ V}$ ramp. This is confirmed also by the C-V curve measured after the $V_G=0-16 \text{ V}$ ramp, showing a positive shift of the flat-band voltage $\Delta V_{FB}=1.6 \text{ V}$. Negligible hysteresis is observed at negative V_G , whereas C-V curves measured after the negative V_G ramp shows a significant $\Delta V_{FB}=-1.6 \text{ V}$, indicating a large hole trapping in the $\text{SiO}_x/\text{Al}_2\text{O}_3$ stack. Despite the same $|\Delta V_{FB}|$ after positive and negative V_G ramps, the larger I-V curve hysteresis observed with $V_G>0$ indicates that electron traps are much slower than hole ones. This result is not affected by the relative sequence of positive and negative I-V. We repeated the same experiment on devices with $t_{\text{Al}}=10 \text{ nm}$. Again, we found that I-V hysteresis is significant especially for positive V_G . C-V curves measured after negative V_G ramp shows a negative $\Delta V_{FB}=-0.76 \text{ V}$, confirming that hole trapping is significant. We investigated also samples with $t_{\text{Al}}=5 \text{ nm}$, observing neither I-V hysteresis nor flat band voltage shift after both positive and negative V_G ramp. This indicates that electron and hole trapping is negligible for t_{Al} thinner than 5 nm. V_{FB} shifts after positive and negative V_G ramps are plotted versus t_{Al} in the inset of Fig. 1. The ΔV_{FB} reduction with decreasing t_{Al} is due to the lower electron/hole charge trapped within the Al_2O_3 stack. Since ΔV_{FB} is negligible for the $t_{\text{Al}}=5 \text{ nm}$ capacitors, we conclude that the charge trapping at the $\text{SiO}_x/\text{Al}_2\text{O}_3$ interface is not dominant. The charge is thus expected to be distributed across the Al_2O_3 volume.

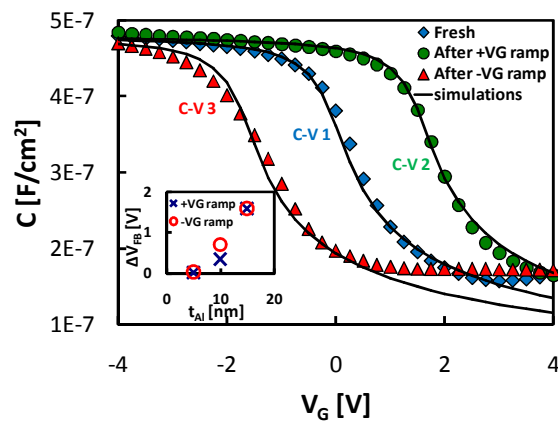


FIGURE 1. C-V CURVES SIMULATED (SOLID LINES) AND MEASURED ON FRESH DEVICE (CIRCLES), AFTER V_G RAMP FROM 0V TO $V_{G,\text{MAX}}$ (TRIANGLES), AFTER V_G RAMP FROM $V_{G,\text{MAX}}$ TO $V_{G,\text{MIN}}$ (SQUARE). THE INSET SHOWS THE ΔV_{FB} MEASURED AFTER POSITIVE AND NEGATIVE V_G RAMPS FOR DIFFERENT ALUMINA THICKNESSES.

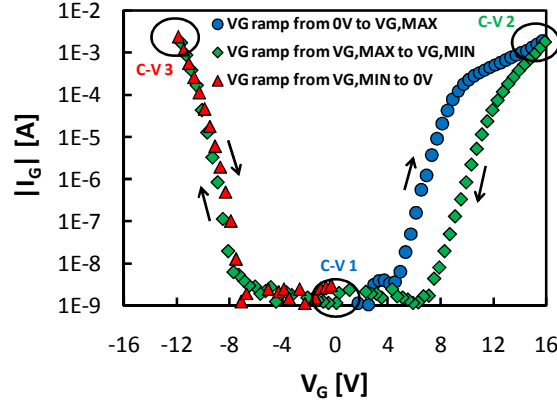


FIGURE 2. I-V CURVES MEASURED ON $t_{\text{Al}}=15 \text{ NM}$ CAPACITORS.

To derive the energy distribution of electron/hole traps we performed retention experiments after positive and negative V_G ramps. ΔV_{FB} curves measured during retention experiments at different temperatures are shown in Fig. 3. The temperature does not affect ΔV_{FB} in retention, see empty symbols, suggesting that charge detrapping is mainly due to tunneling emission rather than thermally activated mechanisms. We use the model in [7] to reproduce the experimental data and to calculate the energy levels for defects. The time evolution of the trapped electron/hole charge is determined by solving self-consistently current continuity and Poisson equations including drift and diffusion mechanisms. Tunneling currents through bottom oxide and alumina blocking layers include direct/FN/modified tunneling contributions, Trap-to-Band Tunneling (TBT) and Trap-Assisted-Tunneling (TAT). Trapping is described according the SRH theory, while detrapping accounts for thermal emission (TE) and TBT contributions. ΔV_{FB} simulations in Fig. 3 performed considering unbiased samples agree very accurately with measurements. Noticeably, a unique set of trap parameters is

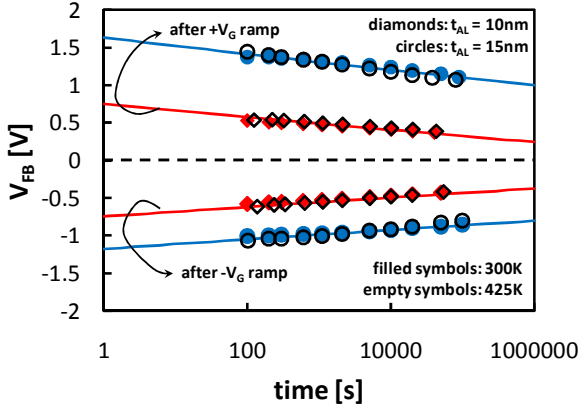


FIGURE 3. IV CURVES MEASURED (SYMBOLS) AND SIMULATED (SOLID LINES) USING THE MODEL IN [2] ON DEVICES WITH $T_{AL}=15\text{nm}$ AND $T_{AL}=10\text{nm}$ AFTER POSITIVE ($\Delta V_{FB}>0$) AND NEGATIVE ($\Delta V_{FB}<0$) V_G RAMPS.

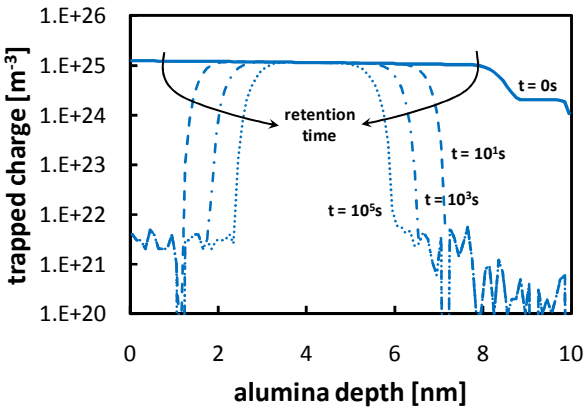


FIGURE 4. ELECTRON CHARGE EVOLUTION DERIVED FROM RETENTION SIMULATIONS ON DEVICES WITH 10 NM THICK ALUMINA.

considered independently of t_{AL} . The energy levels for electrons are deeper ($E_T=2.0\text{-}2.6\text{ eV}$) than hole ones ($E_T=1.6\text{-}2.2\text{eV}$), demonstrating that electron detrapping is slower due to the higher tunneling barrier of trapped electrons. Simulations allow deriving also the location of electron and hole charge inside the Al_2O_3 and its evolution over time in retention, see Fig. 4. As expected, electrons trapped close to the Al_2O_3 interfaces escape immediately, explaining the lower charge found in thinner Al_2O_3 capacitors, i.e. trends of retention and I-V hysteresis measurements.

Charge trapping in Al_2O_3 layer affects TANOS memory operation and reliability, contributing significantly to the V_{FB} shifts in both retention and P conditions. Using the model in [7], we reproduce accurately ΔV_{FB} evolution during program in TANOS devices, see Fig. 5. The charge distribution calculated after program shows a significant electron trapping in the alumina, see Fig. 6. This is also confirmed by the V_{FB} shift observed in retention conditions, performed applying a large gate voltage $V_G=6\text{V}$ to accelerate the charge loss, see Fig. 7. The ΔV_{FB} curve shows a double slope over time well reproduced by simulations, related to the presence of electrons trapped in the alumina layer. Thanks to the much higher tunneling probability, electrons in alumina traps escape much faster compared to electrons in the nitride, determining the double-slope V_T curve. This behavior cannot be reproduced by simulations without considering electron trapping in Al_2O_3 , see dashed line, and is more and more evident with increasing V_G . Simulations show that electron trapping in the alumina can contribute up to the 15% of the total V_{FB} shift.

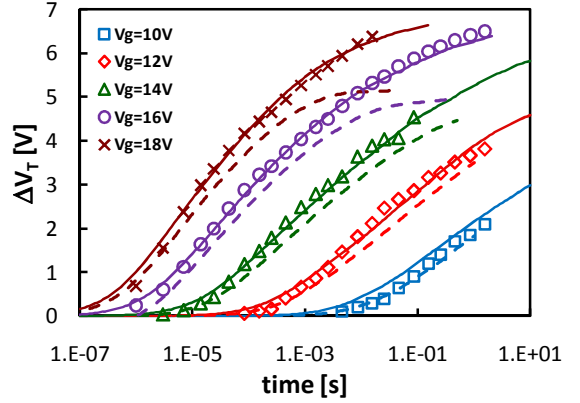


FIGURE 5. I-V CURVES MEASURED (SYMBOLS) ON TANOS CAPACITORS WITH 15NM/4NM/4.5NM ALUMINA/NITRIDE/OXIDE THICKNESSES. SIMULATIONS ARE PERFORMED TAKING INTO ACCOUNT (SOLID LINES) AND NEGLECTING (DASHED LINES) CHARGE TRAPPING INTO THE ALLUMINA LAYER.

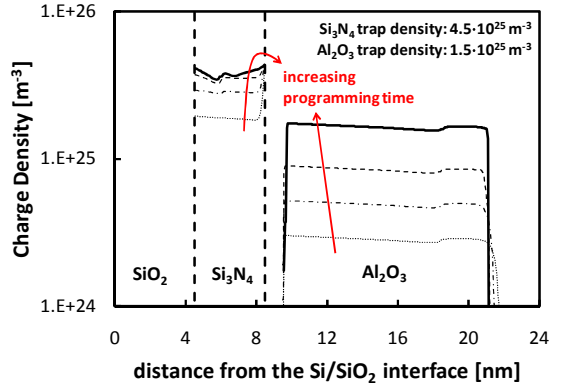


FIGURE 6. ELECTRON CHARGE DISTRIBUTION DERIVED FROM PROGRAM SIMULATIONS PERFORMED WITH THE MODEL IN [2] CONSIDERING A TANOS STACK WITH 4.5/4/15 NM OXIDE/NITRIDE/ALUMINA.

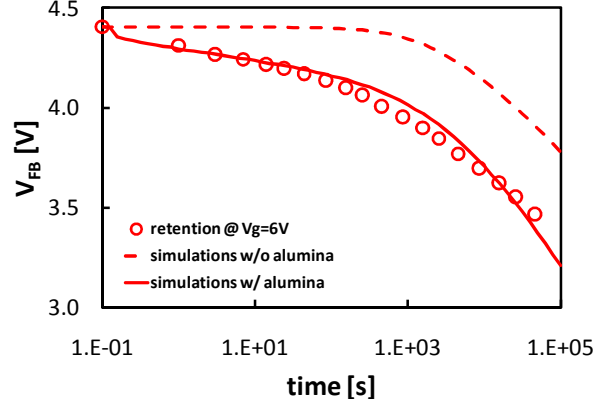


FIGURE 7. ΔV_{FB} MEASURED (SYMBOLS) AND SIMULATED TAKING INTO ACCOUNT (SOLID LINES) AND NEGLECTING (DASHED LINES) ELECTRON TRAPPING IN THE ALLUMINA LAYER IN RETENTION CONDITIONS APPLYING $V_G=6\text{V}$ TO ACCELERATE THE CHARGE LOSS.

REFERENCES

- [1] Y. Park *et al.*, IEDM Tech. Dig., pp. 29-32, 2006.
- [2] J. Robertson, Rep. Prog. Phys. 69, pp. 327-396, 2006.
- [3] T. Sugizaki *et al.*, VLSI Tech. Digest, pp. 27-28, 2003.
- [4] P. Blomme *et al.*, International Memory Workshop, 2009.
- [5] F. Giustino *et al.*, vol. 72, pp. 299-303, 2004.
- [6] L. Larcher *et al.*, IEEE TED, Vol. 48(5), pp.935-945, 2001.
- [7] A. Padovani *et al.*, IEEE EDL, Vol. 30(8), pp. 882-884, 2009.